Hybridization model for the magnetic-ordering behavior of uranium- and cerium-based 1:2:2 intermetallic compounds

T. Endstra, G. J. Nieuwenhuys, and J. A. Mydosh
Kamerlingh Onnes Laboratorium der Rijksuniversiteit Leiden, P.O. Box 9506, 2300 RA Leiden, The Netherlands
(Received 8 June 1992; revised manuscript received 28 April 1993)

It is shown that the occurrence of magnetic ordering in UT_2X_2 and CeT_2X_2 intermetallic compounds, where T denotes a transition metal and X represents Si or Ge, and the magnetic-ordering temperatures in those compounds that order magnetically, are related to the strength of the f-d hybridization. Values for this hybridization strength in various series of such ternary and pseudoternary compounds are obtained via a semiquantitative band-structural approach, and the systematics in these values are used to determine the ordering trends in the phase diagram of a Kondo lattice.

I. INTRODUCTION

An enormous class of ternary intermetallic compounds, and one in which a rich variety of electronic ground states has been observed, is formed by the tetragonal MT_2X_2 compounds. For our purposes M is restricted to uranium or cerium, T denotes a transition metal ($3d$, $4d$, or $5d$), and X is silicon or germanium. Simple Pauli paramagnetism and long-range (anti)ferromagnetic ordering are found in these 1:2:2 compounds, along with the more exotic phenomena associated with "heavy-fermion" behavior, e.g., large effective electron masses, coherence, superconductivity, and the coexistence of superconductivity and antiferromagnetism.

In these compounds, the magnetic moments—if present—are only found on the f atoms, not on the transition metals (the well-known exception being the Mn-containing compounds). Since most of these compounds crystallize in only two allotropic derivatives of the $BaAl_4$ structure (either the body-centered tetragonal $ThCr_2Si_2$ structure, with space group $I4/mmm$, or the primitive tetragonal $CaBe_2Ge_2$ structure, space group $P4/nmm$) they are ideally suited to study the influence of the diverse constituents on the f-electron magnetism. For overviews of the experimental properties of these compounds we refer to Refs. 1–3.

Now that such a large collection of experimental data is available regarding the physical properties of these compounds, we should attempt to confront these data with a theoretical framework. *Ab initio* calculations of the size of the magnetic moments and of the transition temperatures have been carried out by Cooper and co-workers.[4] In their calculational scheme, they have treated both hybridization and Coulomb exchange effects simultaneously in the presence of interconfigurational correlation effects. In this way, they are able to successfully compute the magnetic moments and transition temperatures of a number of U- and Ce-based compounds adopting the NaCl structure. Band-structure calculations[5] are not able to correctly predict these magnetic properties because they include only those aspects of the valence fluctuations that can be captured by time averaging. Therefore, the true character of the $4f$ or $5f$ states is missed and has to be included by adding an additional on-site scattering term[6] or interconfigurational correlation effects.[4] Due to computational limits such calculations have not been carried out for the compounds considered in the present paper. Bearing this in mind, we propose a phenomenological "f-d hybridization model" to account for the systematics in the observed magnetic-ordering temperatures, denoted by T_c for both long-range ferromagnetism and antiferromagnetism. In particular, the nonmonotonic variations found in T_c and the f-d hybridization parameter for the mixed pseudoternary compounds are nicely in accord. Hopefully our simple model will stimulate more theoretical work and new experimental efforts to confirm the validity of the proposed ideas, and will serve as a guideline to roughly predict properties of new materials.

In Sec. II we will introduce the concepts concerning the (magnetic) phase diagram of the Kondo lattice and a simple band-structure approach, which allows us to estimate the hybridization strengths for different compounds. In Sec. III we apply these band-structural concepts to actually calculate the f-d hybridization for various series of MT_2X_2 compounds and, in combination with the phase diagram of the Kondo lattice, use these values to explain the experimentally observed systematic behavior of the magnetic properties of these compounds. Finally, our conclusions are given in Sec. IV.

II. PHASE DIAGRAM OF THE KONDO LATTICE AND THE ROLE OF HYBRIDIZATION

We consider these $(Ce,U)T_2X_2$ compounds as a periodic array of $4f$ (in the case of Ce) or $5f$ (in the case of U) spins in which an indirect, conduction-electron-mediated, magnetic interaction between the local moments is in competition with a Kondo-type spin-compensating mechanism. By comparing the binding energy of a Kondo singlet:

$$k_B T_K \propto N(0)^{-1} e^{-1/N(0)J} \tag{1}$$

with that of a Ruderman-Kittel-Kasuya-Yosida (RKKY) antiferromagnetic state:

$$k_B T_{\mathrm{RKKY}} \propto J^2 N(0) \tag{2}$$

where $N(0)$ is the conduction-electron density of states at the Fermi level, and J an exchange coupling constant, Doniach[7,8] derived a phase diagram for this so-called "Kondo lattice." The stability of the different states in the T-J plane is illustrated in Fig. 1(a). A similar phase diagram was given by Brandt and Moshchalkov[9] for their "concentrated Kondo systems" (CKS) and is shown in Fig. 1(b). Doniach established that at $T = 0$ a second-order phase transition separates the RKKY ground state from the fully spin-compensated ground state (Kondo metal) at a critical value of $J = J_c$. For $J \lesssim J_c$ the ground state consists of magnetically ordered, but partially compensated, f spins. According to Fig. 1, there will always be an initial increase of T_c, the magnetic-ordering temperature, with J. T_c will pass through a maximum and then drop to zero as J is increased above its critical value.

More recent theoretical studies have extended and substantiated these ideas.

(1) The existence of an "instability region" in the phase diagram was indicated, where a pressure-induced first-order phase transition may occur between a mixed and a pure Kondo phase. This idea was applied to explain pressure experiments on Ce and $CeAl_2$.[10]

(2) It was shown that, even for large values of J, magnetic regions can still exist in the phase diagram, depending on the number of conduction electrons. Here an exact equivalence was obtained of the Kondo lattice with infinite J to the Hubbard model with infinite U.[11]

(3) Via the functional integral method[12] or by applying a scaling theory of critical phenomena[13] various authors have studied the "coherence transition" in the Kondo lattice.

(4) The stability of different nonmagnetic (Kondo) and magnetic [RKKY-(anti)ferromagnetic; Nagaoka-ferromagnetic] ground states as a function of the conduction-electron concentration was recently investigated,[14] using a variational method. It was shown that the "lattice enhancement" of the Kondo effect can push the value of J_c to lower values than previously thought.

Although strictly speaking some of the above derivations are only valid for small J/W [$W \propto 1/N(0)$ in the above notation], because of the restricted validity of the Schrieffer-Wolff transformation,[15] there seems to be broad agreement on the general characteristics of the above-sketched phase diagram, both theoretically and experimentally. Particularly, in some dilution and pressure studies on Ce compounds, the predicted transition from local-moment magnetism, via a maximum in magnetic-ordering temperature to a nonmagnetic or reduced-moment state has been confirmed. Examples are the initial increase and subsequent fall of the Curie temperature of ferromagnetic CeAg with hydrostatic pressure,[16] the Curie and Kondo temperatures of $CeNi_xPt_{1-x}$,[17] the characteristics of $CeSi_x$,[18] and the pressure dependence of the Néel temperatures of the CeT_2Si_2 compounds with T=Rh, Pd, Ag, and Au.[19]

We will show that it is possible to use the same phase diagram (Fig. 1) to account for the variation in magnetic-ordering behavior observed in a wide range of (U,Ce)T_2X_2 compounds (X=Si, Ge). Our procedure will be the following: First we determine how the value of J evolves in a given T series [e.g., $U(3d)_2Si_2$ or $Ce(4d)_2Ge_2$], then we place these systems in the phase diagram starting on the left-hand side and in order of increasing J. Finally, we demonstrate that the observed T_c sequences are generally consistent with the phase diagram.

In order to proceed, we must create a conduction-electron–f-electron exchange-interaction parameter J_{cf}; and here we invoke hybridization according to the proportionality

$$J_{\mathrm{cf}} \propto V_{\mathrm{cf}}^2/(E_F - E_f) \tag{3}$$

(see Refs. 20 and 21), where V_{cf} is the hybridization matrix element for conduction-f-electron hybridization and E_f is the location of the f level relative to the Fermi energy E_F. If we take $E_F - E_f$ to be constant in a given transition-metal series, we can, by calculating the conduction-f hybridization of the compounds, obtain an estimate of J_{cf}. It is commonly believed that

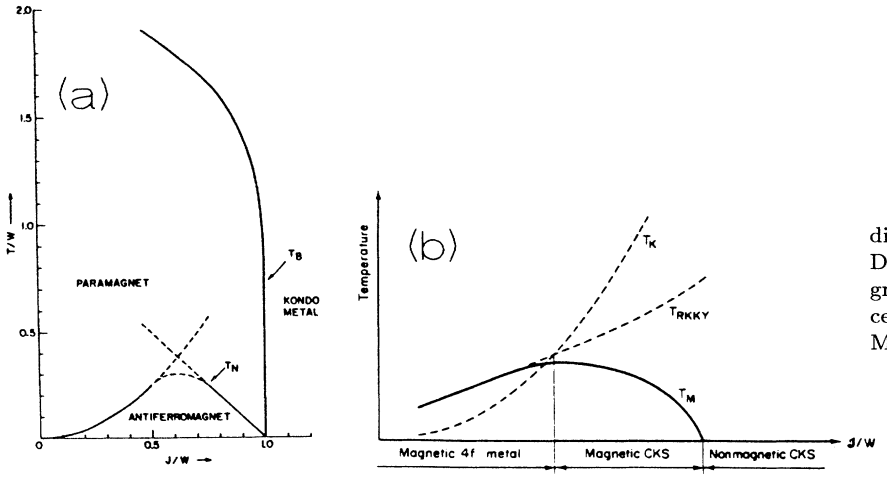

FIG. 1. (a) Phase diagram for the one-dimensional "Kondo-necklace" model [from Doniach (Ref. 7)], and (b) the phase diagram according to a classification of concentrated Kondo systems [from Brandt and Moshchalkov (Ref. 9)].

in these 1:2:2 compounds the hybridization between f states and conduction electrons is mainly governed by f-d hybridization.[22,23] Indeed, our key experimental parameter is the variable number of d electrons, and its effect on T_c. To avoid confusion of terms, we note that our J_{cf} only plays the role of an exchange parameter; it is not the true Coulomb exchange.

Justification for the constant $(E_F - E_f)$ can be obtained from photoemission experiments.[24] These established that the f level is strongly pinned to (just below) the Fermi level, whereas the d band is pulled down in energy, away from the Fermi level with increasing number of d electrons.[24] In the following we assume that the f-d hybridization depends, first, on filling the d band and, second, on the distance between d and f atoms in the crystal structure. Thus, with an increasing number of d electrons the hybridization decreases (less overlap of the d and f bands), which in turn implies a reduction of J_{df}. This reasoning agrees quite well with the simple band model for the $U(3d)_2Ge_2$ compounds as given previously by Dirkmaat *et al.*[22] The second assumption is rather analogous to the Hill criterion,[25] which states that when U-U interatomic distances are too large (larger than 3.5 Å) there will be no direct overlap of the $5f$ wave functions. We now propose that a similar criterion may apply for the U-T interatomic distances, in other words, if $d_{\text{U-}T}$ is too large no f-d hybridization will occur. Consequently, J_{df} will increase both with decreasing number of d electrons and with decreasing U-T separation.

An indication for the relative importance of these two effects can be obtained by following the band-structure approach as put forward by Harrison and Straub.[26–30] (A review of this technique and other tight-binding methods is given in Ref. 31.) The method was initially used to calculate the d-band structure of solids,[26,27] but was later adapted to compute the coupling between atomic orbitals of s, p, d, f symmetry in different compounds.[28–30] This formalism combines Andersen's muffin-tin-orbital (MTO) theory[32] with transition-metal pseudopotentials[26] to obtain a general hybridization ("coupling") matrix element $V_{ll'm}$. From Eq. (B1) of Ref. 30:

$$V_{ll'm} = (\eta_{ll'm}\hbar^2/m_e)[(r_l^{2l-1}r_{l'}^{2l'-1})^{1/2}/d^{l+l'+1}]. \quad (4)$$

The input parameters are the atomic radii of the respective atoms (r_l and $r_{l'}$), the interatomic distance d, the angular momenta l, l' ($l = 0, 1, 2, 3$ for s, p, d, f orbitals), and the symmetry of the bond m. Note that m_e in Eq. (4) is the electron mass. $\eta_{ll'm}$ is given by[30]

$$\eta_{ll'm} = \frac{(-1)^{l'+1}}{6\pi}\frac{(l+l')!(2l)!(2l')!}{2^{l+l'}l!l'!} \times(-1)^m\left(\frac{(2l+1)(2l'+1)}{(l+m)!(l-m)!(l'+m)!(l'-m)!}\right)^{1/2} \quad (5)$$

with $m = 0, 1, 2, 3$ for σ, π, δ, and φ bonds. Such considerations were recently applied to discuss various trends in the hybridization of UTX compounds.[33] The $V_{ll'\sigma}$ matrix elements are the largest ones, other $V_{ll'm}$ equal a numerical constant (<1) times this value. Thus, for describing trends it is sufficient to calculate only these (σ) elements and we will drop the index m. Furthermore, to obtain a real hybridization strength, the number of nearest neighbors should be taken into account, and the contributions of all nearest neighbors should be summed. As long as we restrict ourselves to isostructural compounds with an equal site occupation in the unit cell, this consideration does not play a role. As indicated above the important parameters in determining the f-d hybridization matrix elements are the U-T interatomic distance, and the number of d electrons of the transition metal. The former directly enters into Eq. (4) ($d \equiv d_{\text{U-}T}$) and the latter via the tabulated r_d values.[29] The r_l values with $l = 2$ and 3 (d and f) in Eq. (4) are obtained from fits to known bandwidths of pure metals or from free-atomic data. We have used those values calculated[29] from the MTO bandwidths of the pure d and f metals [see the last columns of Tables I (for d) and II (for f) in Ref. 29]. Moreover, we do not incorporate the V_{pf} (V_{sf}) terms that arise from p-f (s-f) hybridization. Although these terms can be large, they do not change very much within a given T series of compounds, and, thus, are thought not to influence the observed systematics with T as the variable.

We summarize the model with its basic ingredients as applied to the $(Ce,U)T_2X_2$ compounds.

(1) The f-ligand hybridization in these compounds is governed by f-d hybridization, the strength of which is calculated via the "hybridization matrix elements" V_{df} of the Harrison formalism.

(2) The Schrieffer-Wolff transformation [Eq. (3)] is used to relate this hybridization strength to a d-f exchange-coupling parameter J_{df}. The distance of the f level from the Fermi level, $E_F - E_f$, is constant, since the f level is "pinned" to the Fermi energy.

(3) The exchange coupling constant J and a conduction-electron bandwidth W yield the phase diagram (T_c/W vs J/W) as given in Fig. 1, which spans the entire range from local-moment ordering for small J/W to a fully spin-compensated ground state for large J/W. This phase diagram is relevant for the magnetic-ordering properties of these $(Ce,U)T_2X_2$ compounds.

(4) The conduction electrons in these compounds have significant d character. Therefore we examine only f-d hybridization and W represents the d bandwidth.

There are two remarks that should be made with respect to the above protocol. First, the various steps will not (and need not), in general, be *exactly* true, but only represent a first-order approximation. As indicated, they are, to some extent, corroborated by photoemission experiments and general band-structure considerations, however, an exact correspondence cannot be expected. For instance, $E_F - E_f$, W, and the proportionality constant in Eq. (3) can differ somewhat from compound to compound. Nevertheless, we argue that a small (large) value of V_{df} should result in a small (large) J_{df} value, which in turn determines the sequence along the horizontal axis in the Doniach plot (Fig. 1).

The second comment is that from first principles we do not know whether a calculated V_{df} value of a particular compound is to be considered *small* or *large*, i.e., the *absolute* location in the diagram is not directly deduced.

TABLE I. Crystal-structure data, hybridization matrix elements (V_{df}), and magnetic-ordering temperatures (T_c) for UT_2Si_2 compounds. The nature of the magnetic order is given in parentheses after the ordering temperature; the abbreviations denote the type of magnetism as follows: AF antiferromagnetism, FM ferromagnetism, and P (Pauli) paramagnetism. For $CaBe_2Ge_2$ type compounds (indicated by superscript "a") only the shortest $d_{U\text{-}T}$ is given, but an average V_{df} has been calculated by taking into account two different $d_{U\text{-}T}$ distances, see also Ref. 34.

Compound	$d_{U\text{-}T}$ (Å)	V_{df} (eV)	T_c (K)	Ref.
UCr_2Si_2	3.274	0.269	27 (AF)	35
UMn_2Si_2	3.234	0.273	80–100 (FM, U)	36
UFe_2Si_2	3.095	0.320	– (P)	36
UCo_2Si_2	3.100	0.290	90 (AF)	35 and 37
UNi_2Si_2	3.092	0.270	124 (AF)	23 and 37
UCu_2Si_2	3.189	0.204	103–107 (FM)	37
$UCoNiSi_2$	3.091	0.283	115 (AF)	38
$UNiCuSi_2$	3.136	0.237	162 (AF)	38
URu_2Si_2	3.164	0.418	17.5 (AF)	39
URh_2Si_2	3.209	0.354	130–137 (AF)	40 and 41
UPd_2Si_2	3.241	0.308	97, 150 (AF)	40 and 41
UOs_2Si_2	3.179	0.458	– (P)	41
UIr_2Si_2[a]	3.113	0.436	4.9 (AF)	35 and 42
UPt_2Si_2[a]	3.211	0.376	35 (AF)	43
UAu_2Si_2	3.322	0.293	48, 78 (AF ?)	35, 41, and 44

[a]$CaBe_2Ge_2$ crystal structure; others adopt the $ThCr_2Si_2$ structure.

The V_{df} values only become meaningful in a particular *series* of $(Ce,U)(nd)_2X_2$ compounds where a *sequence* of V_{df} values can be calculated. In this way it is possible in many cases—as will be shown below—to derive the *relative* positions of various compounds in a given series, and to correlate the experimentally obtained magnetic temperatures with the predictions of the phase diagram. For example, if in a given series those compounds with the highest calculated V_{df} values are experimentally found to be nonordering (Pauli) paramagnets, there would be agreement with the model, while in the opposite case (high V_{df} values in compounds with strong local-moment magnetic ordering), the model clearly fails to account for the observed phenomena.

As the Ce-based compounds generally order at lower temperatures than their U-based counterparts and as, additionally, *no* simple systematics is observed on changing the X element (this is in agreement with Ref. 20, for isostructural, isoelectronic X substitution in some $CeTX$ compounds), we will describe the $(Ce,U)T_2(Si,Ge)_2$ in four separate series. Note that the vertical (T/W) scales of the curves are also determined in a phenomenological way. Namely, the highest observed magnetic-ordering temperature in a given series of compounds is taken to correspond to the maximum in the phase diagram.

TABLE II. Ordered magnetic moments (μ_{ord}), as observed in neutron-scattering experiments for several UT_2Si_2 compounds. For the *type* of magnetism see Table I.

Compound	μ_{ord} (μ_B/U)	Ref.
UCo_2Si_2	1.42	37
UNi_2Si_2	2.7[a,b]	23
UCu_2Si_2	1.61	37
URu_2Si_2	0.037[b]	47
URh_2Si_2	1.96	40
UPd_2Si_2	3.37[c]	40
UPt_2Si_2	1.67	43

[a]Three magnetic phase transitions were observed, with some ambiguity regarding the lowest-temperature structure and values for the ordered moment.

[b]Spin-density-wave type.

[c]Modulated-amplitude spin structure, in this case the maximum observed value for the ordered moment is given.

III. COMPARISON OF EXPERIMENTAL DATA WITH THE *f-d* HYBRIDIZATION MODEL

A. UT_2Si_2 compounds

In Table I we have collected the U-T interatomic distances, the calculated V_{df} values, and the magnetic-ordering temperatures of the UT_2Si_2 compounds. The first encouraging observation from the entries of the table is that in the series where nonmagnetic compounds are found ($3d$, $5d$) these compounds indeed possess the largest V_{df} values of that series (UFe_2Si_2 and UOs_2Si_2).

The first series we discuss in detail is the $U(3d)_2Si_2$ series of compounds. Considering the crystal-structure data ($d_{U\text{-}T}$) of Table I and the number of d electrons, the following order of increasing V_{df} (and thus J_{df}) can be expected: Cu → Ni → Co → Fe. Namely, in the T=Ni, Co, and Fe compounds the $d_{U\text{-}T}$ are almost equal, implying that the hybridization will solely be determined by the d-band filling. With decreasing number of d electrons this hybridization should increase as discussed above. For T=Cu both the increased distance and the increased d-band filling imply a smaller hybridization, thus complet-

ing the trend. For T=Cr and T=Mn it is not *a priori* clear as to where to put these systems, because lower d-band filling and larger $d_{U\text{-}T}$ have opposite effects. Now Harrison's approach, as discussed above, can be used to calculate the hybridization matrix elements (see Table I). The result confirms the indicated trend, and in addition places the T=Cr and Mn compounds in the sequence in the following way: Cu $\rightarrow$ Cr $\rightarrow$ Ni $\rightarrow$ Mn $\rightarrow$ Co $\rightarrow$ Fe. This sequence can be combined with the presence or disappearance of magnetism according to the associated T_c's as given in Table I. Note that the outcome for UMn_2Si_2 should be regarded as anomalous because of the existence and high-temperature ordering of the Mn moments *in addition* to the U magnetic moments. Here the above picture is too simple and in this case spin-split (magnetic) d bands have to be considered. The results for the $U(3d)_2Si_2$ systems, interpreted in the framework of the Kondo-lattice model, are shown in Fig. 2 together with those for the $U(4d)_2Si_2$ and $U(5d)_2Si_2$ compounds.

The maximum in the curve corresponds to a temperature of $\approx$190 K, which is the highest transition temperature observed in these silicides. It was found in $U(Ru_{1-x}Rh_x)_2Si_2$ with $x = 0.7$.[45] We remark that the apparent agreement of the datapoints with the drawn curve of the phase diagram is somewhat artificial. As indicated above, the model does not yield absolute values of J_{df}/W, nor does it *predict* the ordering temperatures, only the *order* of J, in which we put the systems of a given series into the phase diagram, is given. Yet it is not trivial that this should always work. For instance, the transition temperatures as found in the $U(5d)_2Si_2$ series are consistent with the derived sequence of V_{df} values, whereas if the calculated V_{df} values for UOs_2Si_2 or UIr_2Si_2 would have been smaller than that of UPt_2Si_2 this could (given the ordering temperatures of Table I) never be reconciled with the phase diagram. Thus, in Fig. 2 we relate the *experimentally obtained* magnetic-ordering temperatures (or the absence of magnetic ordering) to the *relative* strength of the f-d hybridization. The values of the f-d hybridization as calculated are only

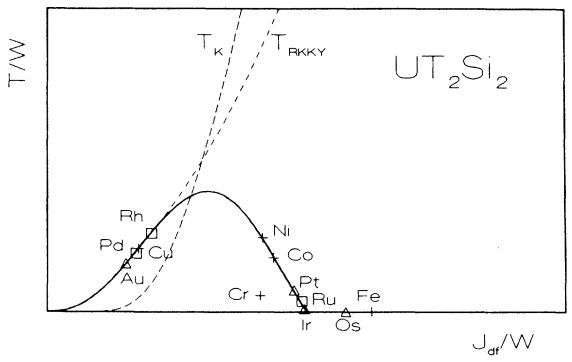

FIG. 2. Schematic phase diagram for the Kondo lattice together with magnetic-ordering temperatures of the UT_2Si_2 compounds. The dashed lines indicate the Kondo and RKKY temperature. The thick line indicates the effective magnetic-ordering temperature in the presence of the Kondo effect. + symbols indicate $3d$ metals, □ is used for $4d$, and △ for $5d$ metals.

comparable for a given set of nd transition metals; hence, a horizontal shift is possible between the different rows of transition metals. It was already mentioned that the systems that do not order magnetically are indeed characterized by the largest V_{df} in a given series (see Table I). Moreover, many of the ordering temperatures are consistent with the derived sequences. In particular, the region around the maximum is interesting. It is clear that, in principle, very high magnetic-ordering temperatures can be obtained when two compounds from both sides of the maximum are alloyed. If the lattice parameters show a monotonic behavior, then the J of a given pseudoternary alloy can be expected to lie in between that of the two boundary compounds. As a consequence the possibility arises of higher-ordering temperatures in the aforementioned case, if the atomic disorder does not destroy the magnetic ordering. This has in fact been used to determine whether UNi_2Si_2 should be placed to the left or to the right of the maximum. Namely, the ordering temperatures of $UCoNiSi_2$ and $UNiCuSi_2$ were determined[38] (see Table I), and it was found that $UNiCuSi_2$ orders at a higher temperature than both parent compounds, whereas $UCoNiSi_2$ orders at a temperature in between that of UNi_2Si_2 and UCo_2Si_2. As shown in Table I the calculated V_{df} values of these alloyed compounds lie in between those of their parent compounds. Not only are these data consistent with the positioning of UNi_2Si_2 to the right of the maximum, but now the observed peculiar behavior of the ordering temperatures, which was previously not understood, follows naturally from the proposed phase diagram.

UMn_2Si_2 is not shown in Fig. 2, but its position between UNi_2Si_2 and UCo_2Si_2 can be considered reasonably in view of the U moments ordering below $\approx$80–100 K. Nevertheless, this may be fortuitous, as in other series the systematics is found not to apply to the Mn compounds with their large Mn moments. This then leaves UCr_2Si_2 as the main exception here, since it should be placed near UNi_2Si_2 in our systematics, but orders at a much lower temperature. Also the absence of any change in the reported ordering temperature of $U(Cu_{1-x}Cr_x)_2Si_2$ with $0 \leq x \leq 0.84$ (Ref. 46) remains unexplained. Whether a local moment exists on the Cr atom is an open question. And the hybridization effect of moving into the left half of the $3d$ series with Cr ($n_d = 4$) is not known.

In the $4d$ series our model does not indicate from first principles whether to place URh_2Si_2 to the left or to the right of the maximum, but alloying studies in the $U(Ru_{1-x}Rh_x)_2Si_2$ system, where very high ordering temperatures are observed on the Rh-rich side[45] (up to $\approx$190 K for $x = 0.7$) indicate positioning of URh_2Si_2, with its ordering temperature of 130 K, on the low-J side. Also no clue is available as to whether UAu_2Si_2 should be placed to the left or to the right of the maximum in the $5d$ series, but parallel to the data on the Ag and Au containing Ce compounds (see below) we chose to display it on the left-hand side of the phase diagram (Fig. 2).

In general one expects to find a full U $5f$ moment in compounds on the left-hand side of the diagram, and re-

duced moments in compounds on the right-hand side. However, it is not at all clear how one should visualize a "magnetic ordering of partially Kondo-screened moments," and whether this could indeed be observed via neutron diffraction. In any case, the effective moments, as seen in the high-temperature susceptibility do not show a systematic difference between compounds from the left- and right-hand sides of the diagram.[34] A comparison of the ordered moments in the magnetic state, as observed in neutron-scattering, is not straightforward, since not all ordered moments are known, many compounds show complicated magnetic order, and the observed magnetic moment at low temperature depends on the crystal-field levels. The compounds for which the magnetic structures and the ordered moments were indeed reported are collected in Table II. No simple trend (e.g., systematic moment reduction with increasing J) is apparent in these ordered moments, although the importance of hybridization effects has been stressed in UPt_2Si_2,[43] and URu_2Si_2 has a strongly reduced magnetic moment.[47]

We remark that typical high-γ compounds, such as URu_2Si_2 and UIr_2Si_2, are located near the magnetic-nonmagnetic border in the phase diagram. Still it is appropriate to emphasize that for a proper treatment of the region where the magnetism disappears, a more sophisticated model is needed, which includes the occurrence of coherence effects[13] and allows for a magnetic transition within the heavy-Fermi-liquid state.[48]

B. UT_2Ge_2 compounds

Unfortunately, in the germanide series less compounds are known to crystallize in $BaAl_4$-type derivatives. In particular, the compounds with T=Cr, Ru, and Os do not exist with the 1:2:2 composition. However, there are two compounds (with T=Co and Ir), where the magnetic properties are known for two different but closely related crystallographic modifications. The results for the UT_2Ge_2 compounds are collected in Table III and shown in Fig. 3. Due to the limited number of compounds in the $4d$ and $5d$ series, the positioning of UPd_2Ge_2 and UPt_2Ge_2 with respect to the maximum cannot be derived. However, the different magnetic-ordering temperatures of the LT and HT (low- and high-temperature) crystallographic phases of UIr_2Ge_2 are consistent with the phase diagram. The T=Rh compound is tentatively put at the transition point between the pure Kondo and mixed Kondo regime where it was previously placed.[55] Note that for the compounds crystallizing in the $CaBe_2Ge_2$ structure no z parameters are available in these germanides. Thus, in these cases the $d_{U\text{-}T}$ values could only be estimated. This was done by calculating the distances as if the compound adopts the more sym-

TABLE III. Crystal-structure data, hybridization matrix elements and magnetic-ordering temperatures for UT_2Ge_2 compounds. Abbreviations as in Table I. "LT" and "HT" denote a low- and a high-temperature crystal-structure modification, respectively.

Compound	$d_{U\text{-}T}$ (Å)	V_{df} (eV)	T_c (K)	Ref.
UMn_2Ge_2	3.364	0.215	100–150 (FM, U)	22 and 36
UFe_2Ge_2	3.199	0.263	– (P)	22 and 36
$UCo_2Ge_2{}^{LT}$	3.182	0.248	174 (AF)	49 and 50
$UCo_2Ge_2{}^{HT\,a}$	3.080[b]	0.302	– (P)	22 and 49
UNi_2Ge_2	3.128	0.251	77 (AF)	22 and 37
UCu_2Ge_2	3.266	0.177	100–110 (FM)	22 and 51
$U(Co_{0.875}Ni_{0.125})_2Ge_2$	3.153	0.259	46 (AF)	34
$U(Co_{0.75}Ni_{0.25})_2Ge_2{}^{a}$	3.134[b]	0.266	19 (AF)	34
$U(Co_{0.5}Ni_{0.5})_2Ge_2{}^{a}$	3.135[b]	0.260	21 (AF)	34
$U(Co_{0.5}Ni_{0.5})_2Ge_2{}^{a}$	3.131[b]	0.262	– (<10)	52
$U(Co_{0.25}Ni_{0.75})_2Ge_2{}^{a}$	3.133[b]	0.255	51 (AF)	34
$U(Co_{0.75}Cu_{0.25})_2Ge_2$	3.199	0.230	130 (AF)	51
$U(Co_{0.5}Cu_{0.5})_2Ge_2$	3.213	0.215	100 (AF)	51
$U(Co_{0.25}Cu_{0.75})_2Ge_2$	3.235	0.197	102 (FM)	51
$U(Ni_{0.75}Cu_{0.25})_2Ge_2$	3.182	0.222	135 (AF)	53
$U(Ni_{0.5}Cu_{0.5})_2Ge_2$	3.213	0.205	140 (AF)	53
$U(Ni_{0.25}Cu_{0.75})_2Ge_2$	3.234	0.192	133 (FM)	53
$U(Ni_{0.1}Cu_{0.9})_2Ge_2$	3.250	0.184	115 (FM)	53 and 54
$URh_2Ge_2{}^{c}$	3.205[b]	0.356		55
UPd_2Ge_2	3.309	0.272	140 (AF)	40
$UIr_2Ge_2{}^{LT\,d}$	3.289[b]	0.346	33 (AF)	56
$UIr_2Ge_2{}^{HT\,a}$	3.194[b]	0.412	19 (AF)	56
$UPt_2Ge_2{}^{a}$	3.261[b]	0.344	72 (AF)	57

[a] $CaBe_2Ge_2$ ($P4/nmm$) crystal structure.

[b] Estimated value; exact z parameters not known.

[c] Exact crystal structure not known.

[d] $Pmmm$ crystal structure.

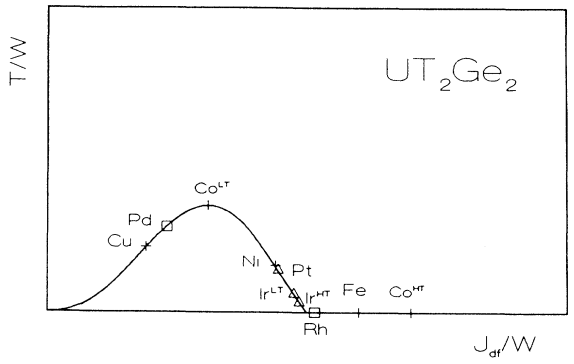

FIG. 3. Schematic phase diagram for the Kondo lattice, with magnetic-ordering temperatures of the UT_2Ge_2 compounds.

metric $ThCr_2Si_2$ structure. A calculation of the V_{df} values of UPt_2Ge_2 and $UIr_2Ge_2{}^{HT}$ by assuming the same z parameters as determined in UPt_2Si_2 and UIr_2Si_2, respectively, yielded slightly different results, but the *order* in the $5d$ series was not affected. The same remains true if one recalculates the values of UIr_2Si_2 and UPt_2Si_2 ($CaBe_2Ge_2$ type) with $ThCr_2Si_2$ structural parameters. In the case of $UCo_2Ge_2{}^{HT}$ the calculated V_{df} is very large due to the short c axis, whichever crystal structure and reasonable set of z parameters are assumed.

In the $U(3d)_2Ge_2$ series, many ternary and pseudoternary compounds have been investigated, so that here a systematic study can be done. First of all it is shown that the existence and disappearance of magnetic order in the case of the two different phases of UCo_2Ge_2 (Ref. 49) fits quite well into the model, i.e., the nonordering (HT) phase has the largest V_{df} value. As $UCo_2Ge_2{}^{LT}$ has a very high T_c, it must be placed at or near the top of the bell-shaped curve. According to the calculated V_{df} sequence in the $3d$ series (see Table III), the T=Cu, Co^{LT}, and Ni compounds should be positioned as shown in Fig. 3. Additional support for this positioning comes from the study of pseudoternary alloys (see also Table III). In particular, high ordering temperatures are found in the $U(Ni_{1-x}Cu_x)_2Ge_2$ compounds by Kuznietz *et al.*[53] Their plot of T_c versus x, in this case, shows a maximum around $x = 0.5$, which is directly related to the maximum in our phase diagram. Upon replacing Co by Cu in $U(Co_{1-x}Cu_x)_2Ge_2$ the ordering temperature decreases[51,52] as expected, but the shallow minimum ($x = 0.5$ and 0.75 samples order at slightly lower temperatures than UCu_2Ge_2, see Table III) is not reproduced by our model. Note that both these series possess the $ThCr_2Si_2$ crystal structure and relatively long c axes. A different situation is encountered in the $U(Co_{1-x}Ni_x)_2Ge_2$ series that *we* have studied.[34] Here rather low ordering temperatures are found, indicating mixing to the right of UNi_2Ge_2. This is consistent with short c axes and the $CaBe_2Ge_2$ type of crystal structure, *and* with the fact that all these alloys show larger V_{df} values than that of UNi_2Ge_2, but smaller than that of $UCo_2Ge_2{}^{HT}$. The initial increase in the calculated hybridization matrix elements V_{df} (see Table III) upon going from $UCo_2Ge_2{}^{LT}$ via $U(Co_{0.875}Ni_{0.125})_2Ge_2$ ($x = 0.125$) to $U(Co_{0.75}Ni_{0.25})_2Ge_2$ ($x = 0.25$) is due to the strongly decreasing $d_{U\text{-}T}$ values, which apparently outweighs the effects due to the increasing Ni content. For larger x, the $d_{U\text{-}T}$ values vary less dramatically, and the increasing d-band filling leads to a decreasing V_{df}. Starting with $UCo_2Ge_2{}^{LT}$, the trend of an initial decrease in T_c (up to $x = 0.25$) and a subsequent increase (for $x > 0.25$) can be followed in the calculated V_{df} values. This is graphically illustrated in Fig. 4. Although there is a striking correspondence, the agreement should not be considered more than qualitative, because the calculated V_{df}'s for UNi_2Ge_2 and UCo_2Ge_2 are too close to explain their largely different ordering temperatures.

Until now the influence of the p-f mixing has been neglected. The importance of this effect, as indicated before, is shown by the fact that no simple systematics can be found upon changing the X element (e.g., Si by Ge). Thus, p-f mixing may play a role especially in the cases where compounds with different structures are compared. However, here the difficulty arises that for many compounds the exact positional parameters of the X element are not accurately determined. In the $U(3d)_2Ge_2$ compounds the Ge coordination of the U atom is almost the same for the compounds crystallizing in the $ThCr_2Si_2$ structure, i.e., each U atom is surrounded by eight Ge nearest neighbors (NN's) at approximately the same distance.[34] The changes in distances and character of the eight transition-metal next-nearest neighbors (NNN's) are much larger, and, as we have argued, this causes the observed variation in magnetic behavior. Whether this reasoning also holds for $CaBe_2Ge_2$ type of compound (e.g., $UCo_2Ge_2{}^{HT}$) is not *a priori* clear because the U coordination changes, and z parameters have not been determined.

C. CeT_2Si_2 compounds

For the T=$3d$ series no magnetic order is found [except for $CeMn_2Si_2$ where the Mn local moments order below 379 K (Ref. 58)]. Therefore, these systems are shown on the nonmagnetic (right-hand) side of the phase diagram given in Fig. 5. Note that the heavy-fermion superconductor $CeCu_2Si_2$ has the lowest V_{df}, and thus lies closest to the magnetic instability in this $3d$ series.

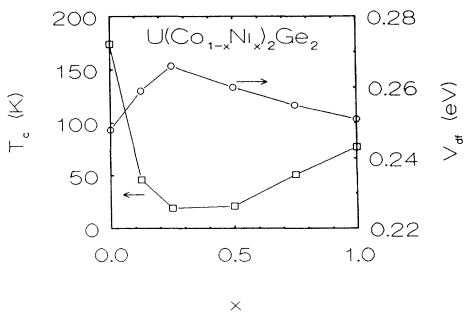

FIG. 4. Magnetic-ordering temperatures (□) and calculated V_{df} values (○) versus x for $U(Co_{1-x}Ni_x)_2Ge_2$ compounds.

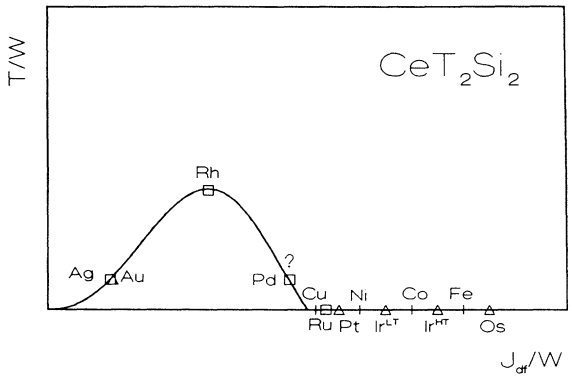

FIG. 5. Schematic phase diagram for the Kondo lattice, with magnetic-ordering temperatures of the CeT_2Si_2 compounds. The question mark attached to Pd is explained in the text.

In the $4d$ and $5d$ compounds the magnetic ordered region is reached for T=Rh, Pd, Ag, and Au (see Table IV). According to our systematics J_{df} should increase as Ag $\rightarrow$ Pd $\rightarrow$ Rh $\rightarrow$ Ru for $T=4d$, and Au $\rightarrow$ Pt $\rightarrow$ Ir^{LT} $\rightarrow$ Ir^{HT} $\rightarrow$ Os for $T=5d$. We remark that for $CeIr_2Si_2$ both a LT and a HT phase (of $ThCr_2Si_2$ and $CaBe_2Ge_2$ types, respectively) exist, neither of which orders magnetically. These systems are shown in Fig. 5. In these series, Severing *et al.*[68] have estimated a consistent set of Kondo temperatures from quasielastic neutron-scattering linewidths. They found the following values for T_K: $CeCu_2Si_2$, 10 K; $CeRu_2Si_2$, 15 K; $CeRh_2Si_2$, 33 K; $CePd_2Si_2$, 10 K; and $CeAu_2Si_2$, 1.7 K. These values should help us in determining positions in the phase diagram (see below). Special difficulties arise in the $4d$ series for T=Rh and Pd. $CeRh_2Si_2$ has the highest ordering temperature of the Ce silicides, and thus sets the scale for this phase diagram. $CeAg_2Si_2$, with the lowest calculated V_{df} value in the $Ce(4d)_2Si_2$ series, should certainly be placed on the left-hand side of the diagram. Now it is difficult to decide whether to place $CePd_2Si_2$ to the left or to the right of the maximum. The large difference (in V_{df} value) between the Ag and Pd compounds with their approximately equal Néel temperature suggests placing them on both sides of the maximum, which is, however, inconsistent with $V_{df}(CePd_2Si_2) < V_{df}(CeRh_2Si_2)$. Hence the question mark in Fig. 5. By dilution experiments Das and Sampathkumaran[69] recently claimed that $CePd_2Si_2$ occupies the top position in Doniach's phase diagram, which is in contradiction to the high ordering temperature of $CeRh_2Si_2$. For T=Ru the nonmagnetic side is reached, and its heavy-fermion characteristics indicate its proximity to the magnetic-nonmagnetic boundary. A qualitatively similar T–J phase diagram was suggested by Severing *et al.*[68] for the CeT_2Si_2 compounds with T=Au, Rh, Pd, Ru (here there was a problem with $CeRh_2Si_2$ whose large T_c was attributed to the larger anisotropy in this system).

Given the above evidence for the very low T_K in $CeAu_2Si_2$, this system should be placed on the left-hand side of the diagram. Then by going to the T=Pt and Ir systems, the rest of the magnetic part of the diagram is skipped, and these are positioned on the nonmagnetic right-hand side, and finally nonmagnetic $CeOs_2Si_2$ nicely completes the $5d$ series.

Last, we mention experiments of Thompson *et al.*[19] on the pressure dependence of the Néel temperatures of CeT_2Si_2 with T=Rh, Pd, Ag, and Au. In $CeAg_2Si_2$ and $CeAu_2Si_2$ it was found that T_c showed only a weak linear dependence on the applied pressure (although of different signs), whereas in $CeRh_2Si_2$ and $CePd_2Si_2$ a strong nonlinear decrease of T_c was observed. Applied pressure can be expected to increase the hybridization, and thus, result in a shift to the right in the phase diagram. The pressure results were indeed interpreted in this way by Thompson *et al.*[19] It was argued that $T_K < T_c$ for T=Ag, Au; the magnetic exchange dominates, and the stable local-moment ordering is hardly influenced by pressure effects. In contrast, for T=Rh, Pd, the opposite holds ($T_K > T_c$), and the increasing strength of the Kondo spin-compensation rapidly suppresses T_c with pressure.

TABLE IV. Crystal-structure data, hybridization matrix elements, and magnetic-ordering temperatures for CeT_2Si_2 compounds. Abbreviations and footnotes as defined in Tables I and III.

Compound	$d_{Ce\text{-}T}$ (Å)	V_{df} (eV)	T_c (K)	Ref.
$CeMn_2Si_2$	3.321	0.181	379 (AF, Mn)	58 and 59
$CeFe_2Si_2$	3.176	0.213	– (P)	59
$CeCo_2Si_2$	3.143	0.208	– (P)	41
$CeNi_2Si_2$	3.131	0.194	– (P)	41
$CeCu_2Si_2$	3.218	0.150	– (P)	60
$CeRu_2Si_2$	3.225	0.290	– (P)	61 and 62
$CeRh_2Si_2$	3.265	0.248	36–39 (AF)	63 and 64
$CePd_2Si_2$	3.256	0.233	8.5–10 (AF)	63 and 65
$CeAg_2Si_2$	3.408	0.164	8–10 (AF ?)	41, 63, and 66
$CeOs_2Si_2$	3.224	0.327	– (P)	62
$CeIr_2Si_2^{LT}$	3.259	0.284	– (P)	62
$CeIr_2Si_2^{HT,a}$	3.217[b]	0.307	– (P)	62
$CePt_2Si_2$[a]	3.246	0.268	– (P)	67
$CeAu_2Si_2$	3.340	0.221	8–10 (AF)	63 and 66

TABLE V. Crystal-structure data, hybridization matrix elements, and magnetic-ordering temperatures for CeT_2Ge_2 compounds. Symbols defined as in previous tables.

Compound	$d_{Ce\text{-}T}$ (Å)	V_{df} (eV)	T_c (K)	Ref.
$CeMn_2Ge_2$	3.426	0.150	316 (FM)	70
$CeFe_2Ge_2$	3.317	0.164	– (P)	71
$CeCo_2Ge_2$	?	?	– (P)	72
$CeNi_2Ge_2$	3.221	0.164	– (P)	73
$CeCu_2Ge_2$	3.296	0.130	4.1 (AF)	74 and 75
$CeRu_2Ge_2$	3.294	0.256	7.5–11 (FM)	76 and 77
$CeRh_2Ge_2$	3.340	0.216	15 (AF)	78
$CePd_2Ge_2$	3.330	0.204	5.1 (AF)	79 and 80
$CeAg_2Ge_2$	3.487	0.143	5–8 (AF?)	76 and 81
$CeIr_2Ge_2$[a]	3.299[b]	0.264	?	82
$CePt_2Ge_2$[a,c]	3.335	0.228	2.2 (AF)	67 and 83
$CeAu_2Ge_2$	?	?	15 (AF)	76

[a] $CaBe_2Ge_2$ ($P4/nmm$) crystal structure.

[b] Estimated value; exact z parameters not known.

[c] A monoclinic variant of the $CaBe_2Ge_2$ structure was reported for this compound in Ref. 83.

D. CeT_2Ge_2 compounds

The properties of this series of compounds are collected in Table V and Fig. 6. For the $3d$ compounds the only Ce magnetic ordering is found for $CeCu_2Ge_2$, the other systems remain nonmagnetic (again with the usual appearance of $3d$ moments in the Mn compound). An indication for the unusual behavior that can be obtained while crossing the magnetic-nonmagnetic boundary is given by the $Ce(Cu_{1-x}Ni_x)_2Ge_2$ pseudoternaries.[84,85] Here a continuous increase in T_K with x was reported, accompanied by drastic changes in the ground-state properties. Successive phases with local-moment ordering, heavy-fermion band magnetism, and heavy Fermi-liquid behavior were identified yielding a very rich phase diagram.[84,85] In the $4d$ series the same problem arises as in the silicides. Namely, it is difficult to determine where the Pd compound should be placed with respect to the top position, which is again determined by the Rh system. To the right it would imply passing two systems with higher V_{df} in view of its ordering temperature, but to the left one would expect (in between the T=Ag and T=Rh compounds) a somewhat higher ordering temperature. In the $5d$ series the lack of experimental data prohibits a systematic treatment with only $CePt_2Ge_2$ being fully characterized. For T=Ir the crystal-structure data are known, but magnetic properties were not reported. In contrast, for T=Au the magnetism was studied without reporting on the crystal-structure data.

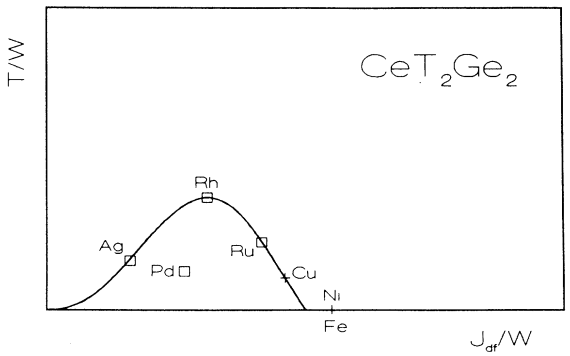

FIG. 6. Schematic phase diagram for the Kondo lattice, with magnetic-ordering temperatures of the CeT_2Ge_2 compounds.

IV. CONCLUSIONS

The systematic behavior of the magnetic properties of $(Ce,U)T_2X_2$ compounds as a function of the transition metal T has attracted considerable experimental attention in the past. However, little theoretical guidance was offered for treating the diversities of the magnetic ordering. Our hybridization model is the first attempt to clarify the mechanism underlying the absence or presence of magnetic ordering *and* the nonmonotonic variation of the magnetic-ordering temperatures of those (ternary and pseudoternary) compounds that do order magnetically.

We have shown that the magnetic-ordering characteristics of the $(Ce,U)T_2X_2$ compounds are determined by the strength of the f-d hybridization. By means of a simple phenomenological band-structure approach we have calculated V_{df} hybridization matrix elements for four different $(Ce,U)T_2X_2$ series of compounds (with X=Si, Ge), and used their relative values within a $(Ce,U)(nd)_2X_2$ series to explain the observed trends, within the Doniach phase diagram for a Kondo lattice. The success of this f-d hybridization model in interpreting the experimental data on these four different 1:2:2 series, may be taken as a strong justification of the initial assumptions. Additional experiments, such as pressure and new pseudoternary compounds are needed to extend the experiment-model comparison.

ACKNOWLEDGMENT

This work was partially supported by the Nederlandse Stichting voor Fundamenteel Onderzoek der Materie (FOM).

[1]A. Szytuła and J. Leciejewicz, in *Handbook on the Physics and Chemistry of Rare Earths, Vol. 12*, edited by K.A. Gschneidner, Jr. and L. Eyring (North-Holland, Amsterdam, 1989), p. 133.
[2]V. Sechovsky and L. Havela, in *Ferromagnetic Materials, Vol. 4*, edited by E.P. Wohlfarth and K.H.J. Buschow (North-Holland, Amsterdam, 1988), p. 309.
[3]T. Endstra, S.A.M. Mentink, G.J. Nieuwenhuys, and J.A. Mydosh, in *Frontiers in Solid State Sciences: Magnetism*, edited by L.C. Gupta and M.S. Multani (World Scientific, Singapore, 1993), p. 167.
[4]B.R. Cooper, Q.G. Sheng, S.P. Lim, C. Sanchez-Castro, N. Kioussis, and J.M. Wills, J. Magn. Magn. Mater. **108**, 10 (1992).
[5]M.R. Norman and D.D. Koelling (unpublished).
[6]P. Fulde, J. Keller, and G. Zwicknagl, in *Solid State Physics*, edited by H. Ehrenreich and D. Turnbull (Academic, San Diego, 1988), Vol. 41, p. 1.
[7]S. Doniach, in *Valence Instabilities and Related Narrow-Band Phenomena*, edited by R.D. Parks (Plenum, New York, 1977), p. 169.
[8]S. Doniach, Physica B **91**, 231 (1977).
[9]N.B. Brandt and V.V. Moshchalkov, Adv. Phys. **33**, 373 (1984).
[10]M. Lavagna, C. Lacroix, and M. Cyrot, Phys. Lett. A **90**, 210 (1982).
[11]C. Lacroix, Solid State Commun. **54**, 991 (1985).
[12]C. Lacroix, J. Magn. Magn. Mater. **63&64**, 239 (1987).
[13]M.A. Continentino, G.M. Japiassu, and A. Troper, Phys. Rev. B **39**, 9734 (1989).
[14]P. Fazekas and E. Müller-Hartmann, Z. Phys. B **85**, 285 (1991).
[15]J.R. Schrieffer and P.A. Wolff, Phys. Rev. **149**, 491 (1966).
[16]A. Eiling and J.S. Schilling, Phys. Rev. Lett. **46**, 364 (1981).
[17]D. Gignoux and J.C. Gomez-Sal, Phys. Rev. B **30**, 3967 (1984).
[18]W.H. Lee, R.N. Shelton, S.K. Dhar, and K.A. Gschneidner, Jr., Phys. Rev. B **35**, 8523 (1987).
[19]J.D. Thompson, R.D. Parks, and H. Borges, J. Magn. Magn. Mater. **54-57**, 377 (1986).
[20]T. Fujita, T. Suzuki, S. Nishigori, T. Takabatake, H. Fujii, and J. Sakurai, J. Magn. Magn. Mater. **108**, 35 (1992).
[21]B. Welslau and N. Grewe, Physica B **165&166**, 387 (1990).
[22]A.J. Dirkmaat, T. Endstra, E.A. Knetsch, A.A. Menovsky, G.J. Nieuwenhuys, and J.A. Mydosh, J. Magn. Magn. Mater. **84**, 143 (1990).
[23]H. Lin, L. Rebelsky, M.F. Collins, J.D. Garrett, and W.J.L. Buyers, Phys. Rev. B **43**, 13 232 (1991).
[24]A. Grassmann, Physica B **163**, 547 (1990); and (unpublished).
[25]H.H. Hill, in *Plutonium and Other Actinides*, edited by W.N. Miner (AIME, New York, 1970), p. 2.
[26]W.A. Harrison, Phys. Rev. **181**, 1036 (1969).
[27]W.A. Harrison and S. Froyen, Phys. Rev. B **21**, 3214 (1980).
[28]W.A. Harrison, Phys. Rev. B **28**, 550 (1983).
[29]G.K. Straub and W.A. Harrison, Phys. Rev. B **31**, 7668 (1985).
[30]W.A. Harrison and G.K. Straub, Phys. Rev. B **36**, 2695 (1987).
[31]J.A. Majewski and P. Vogl, in *Cohesion and Structure, Vol. 2, The Structures of Binary Compounds*, edited by F.R. de Boer and D.G. Pettifor (North-Holland, Amsterdam, 1989), p. 287.
[32]O.K. Andersen and O. Jepsen, Physica B **91**, 317 (1977).
[33]E.H. Brück, Ph.D. thesis, University of Amsterdam, 1991.
[34]T. Endstra, Ph.D. thesis, University of Leiden, 1992.
[35]K.H.J. Buschow and D.B. de Mooij, Philips J. Res. **41**, 55 (1986).
[36]A. Szytuła, S. Siek, J. Leciejewicz, A. Zygmunt, and Z. Ban, J. Phys. Chem. Solids **49**, 1113 (1988).
[37]L. Chełmicki, J. Leciejewicz, and A. Zygmunt, J. Phys. Chem. Solids **46**, 529 (1985).
[38]M. Kuznietz, H. Pinto, H. Ettedgui, and M. Melamud, J. Magn. Magn. Mater. **104-107**, 13 (1992).
[39]T.T.M. Palstra, A.A. Menovsky, J. van den Berg, A.J. Dirkmaat, P.H. Kes, G.J. Nieuwenhuys, and J.A. Mydosh, Phys. Rev. Lett. **55**, 2727 (1985).
[40]H. Ptasiewicz-Bąk, J. Leciejewicz, and A. Zygmunt, J. Phys. F **11**, 1225 (1981).
[41]T.T.M. Palstra, A.A. Menovsky, G.J. Nieuwenhuys, and J.A. Mydosh, J. Magn. Magn. Mater. **54-57**, 435 (1986).
[42]A.J. Dirkmaat, T. Endstra, E.A. Knetsch, G.J. Nieuwenhuys, J.A. Mydosh, A.A. Menovsky, F.R. de Boer, and Z. Tarnawski, Phys. Rev. B **41**, 2589 (1990).
[43]R.A. Steeman, E. Frikkee, S.A.M. Mentink, A.A. Menovsky, G.J. Nieuwenhuys, and J.A. Mydosh, J. Phys. Condens. Matter **2**, 4059 (1990).
[44]L. Rebelsky, M.W. McElfresh, M.S. Torikachvili, B.M. Powell, and M.B. Maple, J. Appl. Phys. **69**, 4810 (1991).
[45]H. Amitsuka and Y. Miyako (unpublished), as cited in H. Amitsuka, T. Sakakibara, Y. Miyako, K. Sugiyama, A. Yamagishi, and M. Date, J. Magn. Magn. Mater. **90&91**, 47 (1990).
[46]K. Hiebl, P. Rogl, C. Horvath, K. Remschnig, and H. Noël, J. Appl. Phys. **67**, 943 (1990).
[47]T.E. Mason, B.D. Gaulin, J.D. Garrett, Z. Tun, W.J.L Buyers, and E.D. Isaacs, Phys. Rev. Lett. **65**, 3189 (1990).
[48]S.M.M. Evans, J. Phys. Condens. Matter **3**, 8441 (1991).
[49]T. Endstra, G.J. Nieuwenhuys, A.A. Menovsky, and J.A. Mydosh, J. Appl. Phys. **69**, 4816 (1991).
[50]M. Kuznietz, H. Pinto, H. Ettedgui, and M. Melamud, Phys. Rev. B **40**, 7328 (1989).
[51]M. Kuznietz, H. Pinto, and M. Melamud, J. Magn. Magn. Mater. **83**, 321 (1990).
[52]M. Kuznietz, H. Pinto, and M. Melamud, J. Appl. Phys. **67**, 4808 (1990).
[53]M. Kuznietz, H. Pinto, H. Ettedgui, and M. Melamud, Physica B **180+181**, 55 (1992).
[54]M. Kuznietz, H. Pinto, H. Ettedgui, and M. Melamud, Phys. Rev. B **45**, 7282 (1992).
[55]A.J. Dirkmaat, T. Endstra, A.A. Menovsky, G.J. Nieuwenhuys, and J.A. Mydosh, Europhys. Lett. **11**, 275 (1990).
[56]B. Lloret, B. Buffat, B. Chevalier, and J. Etourneau, J. Magn. Magn. Mater. **67**, 232 (1987).
[57]T. Endstra, G.J. Nieuwenhuys, A.A. Menovsky, and J.A. Mydosh, J. Magn. Magn. Mater. **108**, 67 (1992).
[58]A. Szytuła and I. Szott, Solid State Commun. **40**, 199 (1981).
[59]P. Rogl, in *Handbook on the Physics and Chemistry of Rare Earths, Vol. 7*, edited by K.A. Gschneidner, Jr. and L. Eyring (North-Holland, Amsterdam, 1984), p. 1, and references therein.
[60]T. Jarlborg, H.F. Braun, and M. Peter, Z. Phys. B **52**, 295 (1983).
[61]L.P. Regnault, W.A.C. Erkelens, J. Rossat-Mignod, P. Lejay, and J. Flouquet, Phys. Rev. B **38**, 4481 (1988).

[62]K. Hiebl, C. Horvath, and P. Rogl, J. Less-Common Met. **117**, 375 (1986).
[63]B.H. Grier, J.M. Lawrence, V. Murgai, and R.D. Parks, Phys. Rev. B **29**, 2664 (1984).
[64]S. Quezel, J. Rossat-Mignod, B. Chevalier, P. Lejay, and J. Etourneau, Solid State Commun. **49**, 685 (1984).
[65]R.A. Steeman, E. Frikkee, R.B. Helmholdt, A.A. Menovsky, J. van den Berg, G.J. Nieuwenhuys, and J.A. Mydosh, Solid State Commun. **66**, 103 (1988).
[66]V. Murgai, S. Raaen, L.C. Gupta, and R.D. Parks, in *Valence Instabilities*, edited by P. Wachter and H. Boppart (North-Holland, Amsterdam, 1982), p. 537.
[67]A. Dommann, F. Hulliger, H.R. Ott, and V. Gramlich, J. Less-Common Met. **110**, 331 (1985).
[68]A. Severing, E. Holland-Moritz, and B. Frick, Phys. Rev. B **39**, 4164 (1989).
[69]I. Das and E.V. Sampathkumaran, Phys. Rev. B **44**, 9711 (1991).
[70]K.S.V.L. Narasimhan, V.U.S. Rao, R.L. Bergner, and W.E. Wallace, J. Appl. Phys. **46**, 4957 (1975).
[71]I. Felner, I. Mayer, A. Grill, and M. Schieber, Solid State Commun. **16**, 1005 (1975).
[72]W.M. McCall, K.S.V.L. Narasimhan, and R.A. Butera, J. Appl. Phys. **44**, 4724 (1973).
[73]G. Knopp, A. Loidl, R. Caspary, U. Gottwick, C.D. Bredl, H. Spille, F. Steglich, and A.P. Murani, J. Magn. Magn. Mater. **74**, 341 (1988).
[74]F.R. de Boer, J.C.P. Klaasse, P.A. Veenhuizen, A. Böhm, C.D. Bredl, U. Gottwick, H.M. Mayer, L. Pawlak, U. Rauchschwalbe, H. Spille, and F. Steglich, J. Magn. Magn. Mater. **63&64**, 91 (1987).
[75]G. Knopp, A. Loidl, K. Knorr, L. Pawlak, M. Duczmal, R. Caspary, U. Gottwick, H. Spille, F. Steglich, and A.P. Murani, Z. Phys. B **77**, 95 (1989).
[76]A. Böhm, R. Caspary, U. Habel, L. Pawlak, A. Zuber, F. Steglich, and A. Loidl, J. Magn. Magn. Mater. **76&77**, 150 (1988).
[77]C. Godart, A.M. Umarji, L.C. Gupta, and R. Vijayaraghavan, J. Magn. Magn. Mater. **63&64**, 326 (1987).
[78]G. Venturini, B. Malaman, L. Pontonnier, and D. Fruchart, Solid State Commun. **67**, 193 (1988).
[79]M.J. Besnus, A. Essaihi, G. Fischer, N. Hamdaoui, and A. Meyer, J. Magn. Magn. Mater. **104–107**, 1387 (1992).
[80]D. Rossi, R. Marazza, and R. Ferro, J. Less-Common Met. **66**, P17 (1979).
[81]U. Rauchschwalbe, U. Gottwick, U. Ahlheim, H.M. Mayer, and F. Steglich, J. Less-Common Met. **111**, 265 (1985).
[82]M. Francois, G. Venturini, J.F. Marêché, B. Malaman, and B. Roques, J. Less-Common Met. **113**, 231 (1985).
[83]I. Das, E.V. Sampathkumaran, R. Nagarajan, and R. Vijayaraghavan, Phys. Rev. B **43**, 13 159 (1991).
[84]F. Steglich, G. Sparn, R. Moog, S. Horn, A. Grauel, M. Lang, M. Nowak, A. Loidl, A. Krimmel, K. Knorr, A.P. Murani, and M. Tachiki, Physica B **163**, 19 (1990).
[85]F. Steglich, U. Ahlheim, C. Schank, C. Geibel, S. Horn, M. Lang, G. Sparn, A. Loidl, and A. Krimmel, J. Magn. Magn. Mater. **84**, 271 (1990).